DuoHexaBody-CD37 induces direct cytotoxic signaling in diffuse large B-cell lymphoma

Simar Pal Singh[1], Michelle D. van den Beukel[1], Sjoerd van Deventer[1], Marije B. Overdijk[2], M. Guy Roukens[2], Kim C.M. Santegoets[2], Esther C.W. Breij[2], Martin ter Beest[1], Annemiek B. van Spriel[1,*]

[1]Department of Medical BioSciences, Radboud Institute for Medical Innovation, Radboud University Medical Center, Nijmegen, the Netherlands.

[2] Genmab, Utrecht, the Netherlands.

[*] Corresponding author: Annemiek van Spriel (annemiek.vanspriel@radboudumc.nl)

Phone number: +31 24317600

Running title: Cytotoxic signaling by DuoHexaBody-CD37

Abstract

Diffuse large B-cell lymphoma (DLBCL) is a common aggressive form of Non-Hodgkin lymphoma. Tetraspanin CD37 is highly expressed on mature B cells and being studied as a therapeutic target for NHL, including DLBCL. DuoHexaBody-CD37 is a biparatopic antibody with an E430G hexamerization-enhancing mutation targeting two non-overlapping CD37 epitopes shown to promote complement-dependent cytotoxicity. However, the impact of DuoHexaBody-CD37 on direct cytotoxic signaling has not yet been studied. Here we demonstrate that DuoHexaBody-CD37 induces direct cytotoxicity in DLBCL-derived tumor cell lines independent of the subtype. DuoHexaBody-CD37 induced significant CD37 clustering and was retained at the cell surface in contrast to rituximab, which was internalized. Unbiased screening identified the modulation of 26 (phospho)proteins upon DuoHexaBody-CD37 treatment of primary B cells or DLBCL cells. Whereas DLBCL cells predominantly upregulated p-SHP1(Y564) upon DuoHexaBody-CD37 treatment, primary B cells showed significantly increased p-AKT(S473) and MAPK signaling which is linked to cell survival. Studies using CD37-mutants identified the N-terminus to be involved in DuoHexaBody-CD37-induced signaling. Finally, DuoHexaBody-CD37 treatment inhibited cytokine pro-survival signaling in DLBCL cells. These findings provide novel insights into the signaling functions of CD37 upon DuoHexaBody-CD37 treatment, and open up opportunities for developing CD37-immunotherapy in combination with small molecule inhibitors to maximize tumor cell death.

Introduction

Diffuse large B-cell lymphoma (DLBCL), an aggressive type of mature B-cell lymphoma, accounts for approximately one third of Non-Hodgkin lymphoma (NHL) cases. DLBCL arises from mature B cells in the lymph node, and comprises a heterogenous group of tumors that can be classified according to cell-of-origin (germinal-center B-cell (GCB) derived and activated B-cell (ABC) subtypes). In addition, recent comprehensive molecular profiling has identified five to seven genetic subtypes that share similar oncogenic pathways [reviewed in [1]]. A large fraction of DLBCL patients (up to 40%) do not respond or relapse after first line treatment with chemotherapy (cyclophosphamide, hydroxydaunorubicin, vincristine sulfate (Oncovin), and prednisone: CHOP) and immunotherapy (rituximab). Rituximab and also next-generation antibodies (ofatumumab) target CD20 at the plasma membrane of DLBCL [2], however decreased expression of CD20 is related to inferior clinical outcome after treatment with R-CHOP [3,4,5]. Thus, targeting alternative B-cell membrane proteins and development of novel immunotherapies are needed to improve clinical outcomes of patients with relapsed/refractory DLBCL [6,7].

CD37 is a tetraspanin protein with four-transmembrane domains, which is predominantly expressed by mature B cells [8–10]. Tetraspanins interact with immune receptors on the same cell (in cis) and control membrane organization in lymphocytes [11–13]. CD37 is absent on progenitor B cells and terminally differentiated plasma cells making it an ideal target for mature B cell malignancies [14,15,16]. In DLBCL patients, CD37 was reported to be an independent prognostic factor for both GCB and ABC subtypes [4]. In line with these findings, CD37-deficient mice show defects in humoral and cellular immune responses, and spontaneously develop mature B-cell lymphoma, which is dependent on IL-6 [17]. IL-6 signals through the IL-6 receptor complex that activates AKT kinase and STAT3 signaling stimulating

64 cell survival and proliferation. IL-6 signaling has been reported to be a critical driver in the
65 tumor microenvironment and a negative prognostic factor in diffuse large B-cell lymphoma
66 [18].

67 CD37 is under preclinical and clinical investigation as novel therapeutic target for B-
68 NHL, including antibody-based and chimeric antigen receptor (CAR) T-cell therapies [19–23,24].
69 DuoHexaBody-CD37 (GEN3009) is a novel biparatopic immunoglobulin G1 (IgG1) with a point
70 mutation in the Fc-domain (E430G) that enhances antibody hexamerization upon binding to
71 the cell surface [25]. This facilitates C1q binding and results in potent complement-dependent
72 cytotoxicity (CDC). In addition DuoHexaBody-CD37 can induce Fc-gamma receptor (FcγR)
73 mediated antibody-dependent cellular cytotoxicity (ADCC) and phagocytosis (ADCP) by
74 effector cells. DuoHexaBody-CD37 mediates superior CDC in patient-derived DLBCL cells ex
75 vivo compared to CD20 monoclonal antibodies as shown in preclinical studies [26].

76 In B cells, CD37 has been reported to connect to intracellular signaling pathways via
77 its two intracellular tails [9,27]. The N-terminal tail of CD37 contains a potential 'ITIM-like' motif
78 that may induce SHP1-dependent cell-death, whereas the C-terminal tail of CD37 bears a
79 predicted 'ITAM-like' motif that may stimulate AKT kinase-dependent survival [27]. Here we
80 investigated whether DuoHexaBody-CD37 is capable of inducing intracellular signaling that
81 induces cell death of malignant B cells. We report that DuoHexaBody-CD37 mediates direct
82 CD37-mediated signaling and evokes tumor cytotoxicity in DLBCL-derived tumor cells,
83 independent of the presence of complement. DuoHexaBody-CD37 modulated the PI3K-AKT
84 and MAPK signaling pathways, with differences observed between primary B cells and DLBCL
85 tumor cells. Moreover, DuoHexaBody-CD37 inhibited IL-4-dependent p-STAT6 and IL-6/ IL-21-
86 dependent p-STAT3 signaling in DLBCL cells. In conclusion, this study shows a novel

87 mechanism of action of DuoHexaBody-CD37, and provides more insight into CD37 as

88 therapeutic target for B cell malignancies.

89

Results

DuoHexaBody-CD37 mediates direct cytotoxicity in DLBCL cell lines

Induction of apoptosis in B cell leukemia and lymphomas has been reported for therapeutic antibodies such as obinutuzumab [28], alemtuzumab [29] and otlertuzumab [30]. To investigate the direct cytotoxic potential of DuoHexaBody-CD37, DLBCL-derived cell lines classified as GCB (Oci-Ly8 and Oci-Ly7), ABC (HBL-1 and U2932) and Burkitt lymphoma-derived cell lines (BJAB, Daudi) were treated with DuoHexaBody-CD37 in the absence of complement, and with or without an Fc-targeting F(ab)2-fragment (a-Fc) to facilitate Fc-mediated crosslinking. Whereas the viability of Burkitt lymphoma-derived cell lines (BJAB and Daudi) was not significantly affected by DuoHexaBody-CD37 treatment with a-Fc, all tested DLBCL-derived cell lines showed >25% reduction in viability after DuoHexaBody-CD37 treatment with a-Fc (Figure 1A). To investigate the physiological relevance of Fc-crosslinking mediated DuoHexaBody-CD37 induced killing, cytotoxicity assays of DLBCL cell lines were performed using peripheral blood mononuclear cells (PBMCs) expressing Fcɣ receptors. In these assays, PBMCs were pre-fixed to prevent FcɣR signaling and to avoid any influence of ADCC/ADCP as previously shown with DuoHexaBody-CD37 [25]. DuoHexaBody-CD37 treatment resulted in significantly increased direct cytotoxicity of DLBCL cells compared to untreated cells in presence of PBMCs as source for Fc-crosslinking for all donors tested (Figure 1B). Collectively, these results show induction of direct cytotoxicity by DuoHexaBody-CD37 treatment with Fc-crosslinking in different DLBCL cells.

DuoHexaBody-CD37 induces CD37 clustering without modulating CD37 cell surface expression

114 CD37 is involved in the spatial organization of the B-cell plasma membrane by forming
115 tetraspanin nanodomains [13], therefore we investigated CD37 membrane clustering on
116 DuoHexaBody-CD37-treated tumor cells compared to tumor cells treated with the IgG1
117 isotype control antibody. Whereas CD37 surface expression was the same in both samples,
118 the clustering of CD37 on tumor cells (measured by fluorescence intensity/area) was
119 significantly higher upon DuoHexaBody-CD37 treatment than isotype control antibody
120 treatment (Figure 2A-B). Interestingly, DuoHexaBody-CD37-mediated clustering of CD37 was
121 observed in both DLBCL (Oci-Ly8) and Burkitt cells (BJAB), even in absence of Fc-crosslinker
122 (Figure 2A-B). Thus, DuoHexaBody-CD37 induces significant CD37 membrane clustering at
123 the cell surface of malignant B cells which is not dependent on Fc-mediated crosslinking.

124 Since the efficacy of rituximab can be negatively impacted by induction of CD20
125 internalization, leading to loss of CD20 expression at the cell surface [31,32], we investigated
126 whether DuoHexaBody-CD37 affected CD37 cell surface accessibility. We observed no
127 changes in surface CD37 expression upon DuoHexaBody-CD37 treatment in all cell lines
128 tested, in contrast to CD20 expression, which was decreased by two-fold on DAUDI, Oci-Ly8
129 and Oci-Ly7 cells upon rituximab treatment (Figure 2C).

130

131 **DuoHexaBody-CD37 treatment results in activation of multiple downstream signaling**
132 **pathways**

133 Next, we focused on investigating mechanisms underlying the direct cytotoxicity upon
134 DuoHexaBody-CD37 treatment by analyzing DuoHexaBody-CD37-induced downstream
135 signaling using high throughput Reverse Phase Protein Array (RPPA) [33]. This technique
136 enables simultaneous unbiased measurement of 484 proteins (102 phospho targets and 382
137 total proteins) in multiple samples at once. For this analysis primary B cells (purified CD19+ B

138 cells from PBMCs) and two DLBCL-derived cell lines (Oci-Ly7 and U2932) were treated with
139 DuoHexaBody-CD37 in the presence or absence of Fc-crosslinker and compared to untreated
140 samples from each cell type. Principal component analysis on all tested proteins in RPPA
141 identified 3 separate clusters correlating with the different cell models (Supplementary
142 Figure 1). Compared to respective untreated controls, 26 phosphoproteins showed >two-fold
143 change in either of the three cell models tested upon DuoHexaBody-CD37 treatment (Figure
144 3A). Pathway analysis on all 26 phospho-sites identified PI3K/AKT/MTOR signaling as the
145 most significantly enriched pathway upon DuoHexaBody-CD37 treatment (Figure 3B). In
146 addition, some of these signaling proteins are downstream of B cell receptor (BCR) signaling
147 and RAS signaling pathways, which have been reported to be essential for B cell survival and
148 lymphomagenesis [34,35].

149 Next, the effect of DuoHexaBody-CD37 treatment on primary B cells versus tumor
150 cells was studied by focusing on those phosphoproteins that showed approximately two-fold
151 upregulation in signal compared to untreated controls. Primary B cells showed upregulation
152 of multiple phosphoproteins upon DuoHexaBody-CD37 treatment including p-AKT, p-FAK, p-
153 Src and p-Shc. In DLBCL cells, different phosphoproteins (p-RPA32, p-DAPK1, p-PAK, p-PI3K
154 and p-FRS-alpha) were upregulated upon DuoHexaBody-CD37 treatment. The list of targets
155 and fold changes can be found in Supplementary Table 1.

156 To validate these results, we analyzed different targets within the three main signaling
157 pathways that came out of the RPPA analysis: the PI3K/AKT pathway, BCR pathway and
158 MAPK/ERK pathway using phosphoflow analysis. Anti-BCR (IgM) was used as stimulation
159 control in the phosphoflow studies. We confirmed specific upregulation of p-AKT(S473) in
160 primary B cells upon treatment with DuoHexaBody-CD37 in the presence of Fc-crosslinker
161 compared to untreated cells (Figure 3C). In DLBCL cell lines, upregulation of p-AKT(S473) was

162 not specific for DuoHexaBody-CD37 treatment as this was already observed in presence of
163 the Fc-crosslinker only (Figure 3C). These data indicate a differential role of DuoHexaBody-
164 CD37 mediated signaling in primary B cells versus DLBCL which could be partially explained
165 by constitutive activation of the PI3K-AKT pathway in DLBCL [36]. As engagement of cell death
166 pathways in CLL cells was shown to be dependent on SHP1 recruitment and activation via
167 CD37 N-terminus [27], we additionally assessed p-SHP1(Y564) status upon DuoHexaBody-CD37
168 treatment of primary B cells and DLBCL cells via phosphoflow. Compared to untreated cells,
169 DuoHexaBody-CD37 treatment in the presence of Fc-crosslinker induced significant
170 upregulation of p-SHP1(Y564) in both primary B cells and DLBCL cells (Figure 3C,
171 Supplementary Figure 2A).

172 To analyze phosphoproteins downstream of the BCR, we studied p-SYK, p-BTK, p-
173 PLCγ2 and p-PKC in primary B cells and DLBCL cells by phosphoflow. p-SYK was observed to
174 be upregulated only after BCR stimulation (anti-IgM), but not after DuoHexaBody-CD37
175 treatment of primary B cells or DLBCL cells (Figure 3C). On other hand, p-PLCγ2(Y759) and p-
176 BTK(Y223) were specifically upregulated in DLBCL cells upon treatment with DuoHexaBody-
177 CD37 in the presence of Fc-crosslinker (Figure 4A, Supplementary Figure 2B). Next, we
178 analyzed the MAPK signaling pathway and observed p-P38 to be specifically upregulated in
179 primary B cells, but not in DLBCL cells, upon DuoHexaBody-CD37 treatment in the presence
180 of Fc-crosslinker (Figure 4B, Supplementary Figure 2C). Similarly, ERK phosphorylation was
181 upregulated in primary B cells upon DuoHexaBody-CD37 treatment in the presence of Fc-
182 crosslinker, in contrast to DLBCL cells (Figure 4B, Supplementary Figure 2C). Taken together,
183 DuoHexaBody-CD37 treatment activates different signaling cascades in primary B cells versus
184 DLBCL-derived tumor cells. Specific upregulation of p-SHP1 in DLBCL cells could provide an
185 explanation of the direct cytotoxicity observed upon treatment with DuoHexaBody-CD37.

186

187 **CD37 N-terminus is involved in DuoHexaBody-CD37-mediated signaling**

188 As tyrosine phosphorylation of the CD37 N-terminus was reported to be crucial in CD37-
189 mediated signaling [27], we examined the involvement of CD37 N-terminus in DuoHexaBody-
190 CD37-induced signaling. In these experiments, B-ALL cells (NALM6) with low endogenous
191 CD37 expression were used to investigate various CD37 mutant constructs [27]. NALM6 cells
192 transfected with wild type CD37 (CD37-WT), or with CD37 carrying either the Tyr13 to
193 phenylalanine mutation (CD37-Y13F) or a deletion of Tyr13 residue (CD37-ΔY13) in the
194 cytosolic region of the CD37 molecule were generated. Cell surface expression of CD37-WT
195 and both mutant variants was validated by flow cytometry (Figure 5A). DuoHexaBody-CD37
196 treatment in the presence of Fc-crosslinker resulted in significant upregulation of p-
197 AKT(S473) and p-SHP1(Y564) in NALM6 cells expressing CD37-WT compared to treatment
198 with only the crosslinker (Figure 5B, C) in line with findings observed in the DLBCL-derived
199 cell lines (Figure 3C). Interestingly, deleting Tyr13 (CD37-ΔY13) completely impaired p-
200 AKT(S473) and p-SHP1(Y564) upregulation, whereas mutating Tyr13 (CD37-Y13F) did not
201 result in major changes upon DuoHexaBody-CD37 treatment in the presence of Fc-crosslinker
202 (Figure 5B, C). In conclusion, these data validate active CD37 downstream signaling upon
203 target engagement with DuoHexaBody-CD37 in the presence of Fc-crosslinker, and suggest
204 the involvement of the CD37 N-terminus in mediating direct cytotoxic signaling.

205

206 **DuoHexaBody-CD37 treatment abrogates cytokine mediated pro-survival signaling in**
207 **DLBCL cells**

208 As cells within the DLBCL tumor microenvironment can stimulate tumor growth by supplying
209 cytokines [37] and CD37 has been reported to inhibit IL-6 signaling [17], we next investigated the

210 impact of DuoHexaBody-CD37 treatment on cytokine-mediated oncogenic signaling.
211 Different DLBCL cell lines were treated with DuoHexaBody-CD37 in absence or presence of
212 Fc-crosslinker, followed by stimulation with either recombinant human IL-4 (rh-IL4), IL-6 (rh-
213 IL6) or IL-21 (rh-IL21) and analyzed for p-STAT activation by phosphoflow. These cytokines
214 were selected because of their pro-tumorigenic role in DLBCL and other hematological
215 cancers [18, 37,38,39,40]. All tested DLBCL-derived tumor cell lines showed a significant increase in
216 the level of p-STAT6 upon rh-IL-4 stimulation. Pre-treatment with DuoHexaBody-CD37 in the
217 presence of a crosslinker showed a significant decrease in percentage p-STAT6-positive tumor
218 cells upon stimulation with rh-IL-4 (Figure 6A) in contrast to controls (untreated or cells
219 treated with DuoHexaBody-CD37 or Fc-crosslinker alone). Next, IL-6-induced p-STAT3
220 signaling was investigated in HBL-1 cells, as the other DLBCL-derived tumor cell lines did not
221 respond to IL-6 (data not shown). A two-fold increase in percentage p-STAT3-positive HBL-1
222 cells was observed upon rh-IL6 stimulation. Interestingly, treatment with DuoHexaBody-CD37
223 in the presence of a crosslinker also decreased the percentage of p-STAT3-positive HBL-1 cells
224 compared to controls (untreated or cells treated with DuoHexaBody-CD37 or crosslinker
225 alone) although this was not significant (Figure 6B). Finally, IL-21-induced p-STAT3 signaling
226 was investigated in all four cell lines. Both ABC-DLBCL derived tumor cells (HBL-1 and U2932)
227 showed a > four-fold increase in the percentage of p-STAT3-positive cells, while the effect
228 was more modest in the GCB-DLBCL-derived tumor cells (Oci-Ly8) showing a two-fold
229 increase in p-STAT3 signal. Oci-Ly7 cells did not respond to IL-21 (data not shown).
230 DuoHexaBody-CD37 treatment in the presence of Fc-crosslinker showed in all three IL-21
231 responsive cell lines a significant decrease in the percentage of p-STAT3-positive cells upon
232 rh-IL21 stimulation (Figure 6C) in line with IL-4 and IL-6 stimulation. Collectively, these

233 experiments show that DuoHexaBody-CD37 treatment in the presence of Fc-crosslinker

234 inhibits cytokine-mediated pro-survival signaling in the DLBCL tumor microenvironment.

235

236 ## Discussion

237 A large fraction (~40%) of patients with DLBCL do not respond to or relapse after first-line
238 treatment with standard immunochemotherapy (R-CHOP), emphasizing the unmet medical
239 need to develop new therapies for DLBCL. Tetraspanins have gained strong interest as
240 therapeutic targets in different cancer types due to their capacity to regulate cell
241 proliferation, adhesion and migration. Importantly, many tumor cells have altered cell
242 surface expression of tetraspanins making them attractive targets for the treatment of cancer
243 [16,41]. For example, CD151 is upregulated in carcinomas and CD151 stimulates both primary
244 tumor growth and the metastatic cascade through its interaction with β1 integrins [41,42]. In B
245 cell lymphoma, CD81 has been reported to be highly expressed by malignant cells from
246 patients with B-NHL, and CD81-specific antibodies have been reported to be cytotoxic for
247 such cells while sparing normal B cells [43]. CD37 represents an alternative therapeutic target
248 for B-NHL because of its specific membrane expression on mature B cells, and its prognostic
249 value in DLBCL and follicular lymphoma [4,44]. DuoHexaBody-CD37 has been previously
250 reported to mediate cytotoxicity of DLBCL cells via different mechanisms of action:
251 complement (CDC) and effector cell-mediated killing (ADCC/ADCP) [25,26]. Here, we report an
252 additional mechanism of action of DuoHexaBody-CD37: CD37-mediated direct cytotoxicity
253 which is independent of complement. Direct antibody-mediated killing may be particularly
254 important in the DLBCL tumor microenvironment when complement is not available or
255 inhibited. Complement has a dual role in tumors including hematological malignancies. The
256 protective role of complement in antibody-mediated CDC has been well-established.
257 However, more recent studies have provided evidence that tumors can hijack the
258 complement components by cell surface expression of C1q, C3a and C5a receptors that
259 promotes tumor growth and progression [45,46]. In addition, lymphoma cells can upregulate

260 complement regulatory proteins (CRPs: CD46, CD55 and CD59) to escape from antibody-
261 mediated CDC [47]. Although no direct correlation was found between DuoHexaBody-CD37-
262 induced CDC and expression of CRPs in vitro [26], expression of CD59 has been shown to
263 predict clinical outcome in DLBCL patients treated with R-CHOP [48]. In addition, the presence
264 of regulatory myeloid cells (tumor-associated neutrophils, myeloid-derived suppressor cells)
265 in the tumor microenvironment has been associated with immune suppression and poor
266 prognosis in lymphoma (reviewed in [37,49]). These tumor-infiltrating myeloid cells stimulate
267 tumor growth and may impair ADCC/ADCP activity of therapeutic antibodies [50]. Lastly, DLBCL
268 cells have been shown to upregulate CD47 to protect themselves from ADCC and ADCP [51].
269 Taken together, inhibition of complement activation by tumor cells or ineffective ADCC/ADCP
270 may limit efficacy of antibody-based immunotherapies for hematological malignancies.

271 Since decreased expression of CD20 is related to inferior clinical outcome of DLBCL
272 patients after treatment with R-CHOP, DuoHexaBody-CD37 treatment may be more potent
273 compared to CD20-targeting therapies in DLBCL. Supporting this, we observed no/minimal
274 internalization of CD37 by DuoHexaBody-CD37 in contrast to rituximab-induced CD20
275 internalization. We observed that DLBCL cells were more sensitive to DuoHexaBody-CD37-
276 mediated cytotoxicity than Burkitt cells, a difference that cannot be explained by variations in
277 CD37 surface expression or clustering. It is possible that Burkitt cells rely on other oncogenic
278 signaling pathways (i.e. MYC-driven) compared to DLBCL cells.

279 The activation of multiple intracellular signaling pathways, including PI3K-AKT and
280 RAS-MAPK that play a central role in cancer, was observed upon DuoHexaBody-CD37
281 treatment of DLBCL cells. This was dependent on Fc-crosslinking of DuoHexaBody-CD37,
282 which is in line with former studies using CD37-specific small modular
283 immunopharmaceuticals (CD37-SMIP) [52,53]. In vivo crosslinking could be facilitated by

284 effector cells expressing Fc receptors, as evidenced by the observed direct cytotoxicity of
285 DuoHexaBody-CD37 in tumor cells in the presence of PBMCs. This did not require FcγR-
286 mediated signaling or effector cell function (degranulation, trogocytosis) as fixed PBMCs
287 could be used to facilitate the crosslinking. CD37 can activate and inhibit AKT kinase through
288 its two intracellular tails that contain ITIM-like and ITAM-like motifs [27]. Different mechanisms
289 of direct tumor cell death by antibodies have been reported, including apoptosis, necrosis,
290 pyroptosis and necroptosis, and future studies are required to identify which of these
291 mechanisms underlie DuoHexaBody-CD37-induced killing of DLBCL cells. Interestingly,
292 increased p-AKT was observed in primary B cells upon DuoHexaBody-CD37 treatment in
293 contrast to malignant B cells, indicating that primary B cells may be less sensitive to direct
294 killing than lymphoma cells. Our results show that DuoHexaBody-CD37 directly affects
295 membrane-proximal signaling proteins (AKT and SHP-1) which provides new opportunities
296 for combination therapies in DLBCL [54]. For example, studies combining CD37-targeting
297 antibodies with PI3K inhibitors [55,56] or cell cycle kinase inhibitors [57] demonstrated enhanced
298 tumor cell death. We also observed p-BTK and p-PLCy upregulation in ABC-DLBCL upon
299 DuoHexaBody-CD37 treatment, which could provide a rational to combine DuoHexaBody-
300 CD37 with ibrutinib in ABC-DLBCL where BTK inhibition is already more effective compared to
301 GBC-DLBCL [58,59].

302 Moreover, DuoHexaBody-CD37 was found to be particularly effective in
303 downregulating p-STAT3 and p-STAT6 in presence of IL-6, IL-21 and IL-4, respectively. Within
304 the DLBCL tumor microenvironment, these cytokines actively contribute to cancer
305 pathogenesis in ABC-DLBCL [18,37,38,39,40]. IL-6 levels in serum are associated with adverse
306 clinical outcome in DLBCL, and we previously reported that CD37 inhibits IL-6 receptor
307 signaling through SOCS3 [17]. In line with this, patients with CD37-negative DLBCL present with

308 higher IL-6 levels in serum and tumors which is associated with inferior clinical outcome [17].
309 CD37 is an independent prognostic factor in DLBCL, irrespective of DLBCL subset [4], which has
310 been confirmed in patients with follicular lymphoma [44]. We anticipate that targeting CD37,
311 especially in the presence of classical chemotherapy and/or targeted drugs will further
312 enhance the efficacy of immunotherapy of DLBCL. In conclusion, this study shows
313 DuoHexaBody-CD37 induces cytotoxic signaling in DLBCL cells, and reduces cytokine-
314 mediated pro-survival signaling in the DLBCL tumor microenvironment.
315
316
317
318
319
320
321
322

323 # Material and Methods

324 **Therapeutic antibodies**

325 DuoHexaBody-CD37 (GEN3009) and the negative control anti-HIV-1 gp120 antibody IgG1-b12
326 (mentioned in manuscript as IgG1-ctrl) were generated by Genmab (Utrecht, The
327 Netherlands) as previously described [60]. Rituximab anti-CD20 (Mab Thera®) was obtained
328 from Radboudumc (Nijmegen, the Netherlands).

329

330 **Cell culture**

331 Lymphoma cell lines (GCB-DLBCL: Oci-Ly8, Oci-Ly7; ABC-DLBC: HBL-1, U2932; B-ALL: NALM6,
332 and Burkitt: BJAB, DAUDI) were obtained from DSMZ, ATCC and Blanca Scheijen (Dept.
333 Pathology, Radboudumc) and cell lines were authenticated using STR-analysis. Cells were
334 cultured in RPMI 1640 (Gibco), 1% antibiotic-antimycotic (Gibco) and 10% FBS (Hyclone)
335 (RPMI/10%FCS) and incubated at 37°C with 5% CO_2. For optimum growth, the cell lines were
336 propagated in dilution of 0.5×10^6 cells/ml and the culture media were refreshed twice a
337 week. All experiments were performed one day after refreshing medium and expanding cell
338 culture.

339

340 **MTS assay**

341 Cell viability was determined using CellTiter 96® AQueous One Solution Reagent from
342 Promega as per manufacturer instructions. Briefly, $2x10^5$ cells in RPMI/10%FCS were plated
343 in 96-well plates and treated with 5μg/ml DuoHexaBody-CD37 for 30min at 4°C. Cells were
344 washed and treated with 5μg/ml of goat F(ab')2 anti-human IgG (a-Fc, Southern Biotech)
345 and incubated for 48h at 37°C with 5% CO_2. As control, cells treated with DuoHexaBody-
346 CD37 or a-Fc alone were included. Subsequently, cells were stained with 1:5 dilution of

347 CellTiter 96® AQueous One Solution Cell Proliferation Assay (MTS, Promega) in media
348 (RPMI/10%FCS) and incubated at 37°C with 5% CO_2 for 2-3h. Absorbance was recorded at
349 490nm in a 96-well plate reader (Bio-Rad iMark Microplate Absorbance Reader).
350
351 **Cytotoxicity assays**
352 Peripheral blood from healthy volunteers was obtained via Sanquin blood bank (Nijmegen,
353 NL) upon informed consent and anonymized for further use, following the guidelines of the
354 Institutional Review Board, and in accordance with the declaration of Helsinki. Peripheral
355 blood mononuclear cells (PBMCs) were isolated using Ficoll Hypaque (GE Healthcare, Little
356 Chalfont, UK) according to the manufacturer's instructions. For fixation, PBMCs were washed
357 with PBS and resuspended directly in 1%PFA (filter sterilized) at $7.5x10^6$ cells/ml for 20min at
358 RT (room temperature). Following, cells were washed twice in PBS and resuspended in media
359 (RPMI/10%FCS). In parallel, $10x10^6$ target cells (HBL-1 or U2932) were stained with CellTrace
360 Violet Cell Proliferation Kit (Invitrogen) at final concentration of 167nM for 20min at 37°C
361 with 5% CO_2. Subsequently, cells were washed twice and resuspended in media
362 (RPMI/10%FCS). Next, CTV-stained target cells were treated with 5μg/ml DuoHexaBody-
363 CD37 for 30min at 4°C and washed with media. In addition, target cells were co-cultured
364 with fixed PBMCs at 1:20 (target to crosslinker) ratio for 4, 24 or 48h at 37°C in the presence
365 of 5% CO_2. Subsequently, cells were directly stained with 5μg/ml propidium iodide (Miltenyi
366 Biotec) for 5min at RT on plate shaker and analyzed using FACS Lyric (BD Biosciences).
367
368 **Target binding analysis**
369 Briefly, 100,000 lymphoma cells (HBL-1, Oci-Ly7, U2932, BJAB or DAUDI) were treated with
370 5mg/ml of anti-CD20 Rituximab (Mab Thera®) or DuoHexaBody-CD37 in RPMI/0.2%BSA for

371 15min at RT in a 96-wells plate. Plates were then directly transferred to incubator (37°C/5%
372 CO_2) for 0, 2 or 6h. Cells were harvested at respective time points by washing with PBA buffer
373 (PBS, 1% BSA, azide 0.02%) followed by staining with mouse anti-human IgG1 Fc secondary
374 antibody conjugated to Alexa Fluor 488 (ThermoFisher) for 30min at 4°C. Next, cells were
375 washed and stained with Live-dead marker (eFluor 506, eBioscience) and measured using
376 FACS Lyric (BD Biosciences).
377
378 **Generation of CD37 mutant cell lines**
379 NALM6 cells were used because of their endogenous low CD37 expression. Cells were grown
380 in RPMI/10% FBS supplemented with glutamine 2mM. Cells were transfected with either
381 CD37-sGFP2, CD37 Y13F-sGFP2 or CD37-delta Y13-sGFP2 constructs using the Amaxa 4D
382 nucleofector. Briefly, for each transfection $3x10^6$ cells were collected and washed with PBS.
383 Cells were resuspended in 100 µl SF buffer (cat. no. V4XC-2024) containing 3 µg of plasmid
384 and pulsed with program CV-104. After transfection, cells were transferred to 6-well plates
385 and incubated overnight in 3 ml of RPMI with 10% FBS without antibiotic-antimycotic and
386 phenol red. The CD37 constructs were kindly provided by Prof. Dr. N. Muthusamy (Ohio
387 University, USA) [27], and subcloned in pSGFP-N1 vector using standard techniques. Sequences
388 were verified via sequencing.
389
390 **Phosphoflow assays**
391 Lymphoma cells ($2x10^5$ cells/well) or PBMCs ($5x10^5$ cells/well) in RPMI/10%FCS were treated
392 with 5µg/ml DuoHexaBody-CD37 for 30min at 4°C. Next, cells were washed and treated with
393 5µg/ml of goat F(ab')2 anti-human IgG (a-Fc) and incubated for 20min at 37°C with 5% CO_2.
394 As treatment control, cells were treated with DuoHexaBody-CD37 or a-Fc alone. As positive

395 control of B-cell receptor stimulation, cells were treated with 20µg/ml of goat F(ab')2 anti-
396 human IgM. Next, cells were spun down and stained at 1:10 dilution with Fixable Viability
397 stain 510 (BD Biosciences) in RPMI/10%FCS for 10min at 37°C. Thereafter, cells were directly
398 fixed for 10min at 37°C with 100 µl of the eBioscience FoxP3/Transcription Factor Fixation kit
399 (Invitrogen) as indicated by the manufacturer. After fixation, samples were washed twice
400 with eBioscience Permeabilization Wash Buffer (10X diluted in Milli-Q) (Invitrogen). To
401 identify the B cells within PBMC cultures, cells were stained with antibodies against CD19,
402 CD3 and IgD diluted in eBioscience wash buffer. To prevent non-specific antibody binding,
403 FcR-blocking purified rat anti-mouse CD16/CD32 (Mouse BD Fc BlockTM) was included in the
404 staining. Stained cells were incubated for 30min at 4°C followed by washing in eBioscience
405 wash buffer and staining with antibodies against phosphorylated proteins; p-SHP1(Y564), p-
406 AKT(S473), p38(T180/Y182) (all Cell signaling technology), p-SYK(Y348), p-BTK(Y223), p-
407 PLCy2(Y759), p-PKCα/βII(T638/641), p-ERK-1/2(T202/Y204) (all BD Biosciences); in wash
408 buffer for 30min at RT. Unlabeled phospho-antibodies (p-SHP1(Y564), p-AKT(S473),
409 p38(T180/Y182)) were stained with a secondary PE-labeled F(ab')2 donkey anti-rabbit IgG
410 (H+L) antibody (Jackson Immuno Research) for 15min at RT. Lastly, the cells were washed and
411 resuspended in wash buffer before measuring on FACS Lyric.
412

413 **Cytokine stimulation experiments**

414 To measure p-STAT3 and p-STAT6 responses, cells treated with DuoHexaBody-CD37 and/or
415 goat F(ab')2 anti-human IgG (a-Fc) for 24h as described above. After washing, cells were
416 stimulated with recombinant IL-6 (100ng/ml) or IL-4 (20ng/ml) (both from Miltenyi) or IL-21
417 (Peprotech) (50ng/ml) for 15min at 37°C. Cells were harvested and stained with Fixable
418 Viability stain 510 (BD Biosciences). Subsequently, cells were fixed with BD Cytofix Fixation

419 Buffer (BD Biosciences) for 10min at 37°C and washed twice with MACS buffer (PBS/0.5%
420 BSA/2 mM EDTA). Next, cells were permeabilized using 150 µl Perm Buffer III (BD
421 Biosciences) at 4°C for 30min and washed twice with MACS buffer, followed by staining with
422 PE-labeled p-STAT3 (Y705) or p-STAT6 (Y641) (BD Biosciences) antibody diluted (1:8) in MACS
423 buffer for 30min at RT. Finally, the cells were washed and resuspended in 50 µl MACS buffer
424 before measuring on FACS Lyric.
425
426 **Supplementary methods:** Microscopy analysis of CD37 clustering and RPPA assay
427

Acknowledgements

We thank the Radboudumc Microscopy Imaging Center for use of their microscopy facilities, as well as for their support and assistance. We thank Simone Oostindie and Inge Verbrugge for valuable scientific input, and Peter Friedl for facilitating the RPPA studies. The CD37 constructs were kindly provided by Natarajan Muthusamy (Ohio University, USA) [27].

Disclosures

MGR, MBO, KCMS and ECWB are Genmab employees and own Genmab warrants and/or stock. All the other authors have no conflicts of interest to disclose. This research study was funded by Genmab, and ABvS is supported by the Netherlands Organization for Scientific Research (NWO): the Institute of Chemical Immunology (project ICI00023), ZonMW (project 09120012010023), the Dutch Cancer Society (projects 12949 and 14726), and the European Research Council: Consolidator Grant (project 724281) and Proof-of-Concept Grant (project 101112687).

Author contributions

ABvS, SPS, ECWB, MGR, KCMS and MBO provided scientific input and conceptualized the study. SPS developed the methodology and performed the data analysis for the cytotoxicity assays, PBMC assays, phosphoflow experiments, CD37 mutant studies, cytokine studies and RPPA analysis. MDvdB performed the surface accessibility assays and CD37 mutant studies. SvD developed the methodology for the CD37 transfections. MTB developed methodology of CD37 microscopy studies and performed data analysis on CD37 clustering. SPS and ABvS

wrote the manuscript. ABvS supervised the study. All authors read, revised, and agreed on the final version of the manuscript.

453 # Figure legends

454 **Figure 1: DuoHexaBody-CD37-induces direct cytotoxicity in DLBCL-derived tumor cell lines**

455 **(A)** Percentage decrease (mean +/- SD) in viability upon DuoHexaBody-CD37 treatment in
456 presence or absence of goat F(ab')2 anti-human IgG (a-Fc) in indicated cell lines after 48h.
457 Data is shown from at least three independent experiments. Significance was calculated
458 compared to untreated control using Kruskal-Wallis test followed by Dunn' multiple
459 comparison test correction (**p<0.01) **(B)** Percentage increase in cell death (PI-positive)
460 upon co-culturing healthy donor-derived fixed PBMCs with DuoHexaBody-CD37 pre-treated
461 HBL-1 and U2932 cells compared to untreated cells for indicated time points. Duplicates from
462 each individual donor (n=4) are indicated in separate colors. Significance was calculated
463 compared to 4h treated cells using Kruskal-Wallis test followed by Dunn' multiple
464 comparison test correction (*p<0.05, **p<0.01, ***p<0.001).

465

466 **Figure 2: DuoHexaBody-CD37 induces CD37 clustering without modulating CD37 cell**
467 **surface expression**

468 **(A,B)** Airyscan images depicting clustering (fluorescence/area) upon DuoHexaBody-CD37
469 (DHB) treatment or B12 isotype control in BJAB **(A)** and Oci-Ly8 **(B)** cells. Data shown from
470 three independent experiments. Bar is 10 μm. Significance was calculated comparing
471 DuoHexaBody-CD37 treated cells to isotype control antibody using unpaired T-test
472 (****p<0.0001). **(C)** Percentage decrease (mean +/- SD) in cell surface binding by
473 DuoHexaBody-CD37 or rituximab in indicated cell lines as measured by flow cytometry. Data
474 is shown from at least three independent experiments. Significance was calculated
475 comparing respective time point using unpaired T-test (*p<0.05, **p<0.01, ***p<0.001).

476

477 **Figure 3: DuoHexaBody-CD37 treatment results in activation of different downstream**
478 **signaling pathways**

479 (**A**) Heatmap depicting log-normalized signal intensities of 26 phosphoproteins with two-fold
480 increase in signal upon DuoHexaBody-CD37 treatment in presence or absence of goat F(ab')2
481 anti-human IgG (a-Fc) in primary B cells, U2932 and Oci-Ly7. (**B**) Oncogenic hallmark
482 signatures obtained from the MSigDB enriched using 26 phosphoproteins with two-fold
483 increase in signal upon DuoHexaBody-CD37 treatment in presence or absence of goat F(ab')2
484 anti-human IgG (a-Fc) in primary B cells, U2932 and Oci-Ly7. (**C**) Phosphoflow analysis of p-
485 SYK(Y348), p-SHP1(Y564), p-AKT(S473) on primary B cells (*top row*) or DLBCL cells (*bottom*
486 *row*) either untreated or treated with anti-BCR (F(ab')2 anti-IgM), DuoHexaBody-CD37
487 and/or goat F(ab')2 anti-human IgG (a-Fc). Dot plots depict quantification (mean +/- SD) of
488 mean fluorescence intensity (MFI). Each dot represents individual donor (B cells) or
489 experimental replicate (DLBCL). Significance was calculated compared to untreated control
490 using Kruskal-Wallis test followed by Dunn' multiple comparison test correction (**p<0.01,
491 ***p<0.001, ****p<0.0001).

492

493 **Figure 4: DuoHexaBody-CD37 treatment results in differential activation of BCR and**
494 **RAS/MAPK downstream signaling proteins in primary B cells and DLBCL**

495 (**A, B**) Phosphoflow analysis of (A) p-BTK(Y223), p-PLCγ2(Y759), p-PKCα/βII(T638/641) and (B)
496 p38(T180/Y182), p-ERK-1/2(T202/Y204) on primary B cells (*top row*) or DLBCL cells (*bottom*
497 *row*) either untreated or treated with anti-BCR (F(ab')2 anti-IgM), DuoHexaBody-CD37
498 and/or goat F(ab')2 anti-human IgG (a-Fc). Dot plots depict quantification (mean +/- SD) of
499 mean fluorescence intensity (MFI). Each dot represents an individual donor (primary B cells)
500 or experimental replicate (DLBCL tumor cell lines). Significance was calculated compared to

501 untreated control using Kruskal-Wallis test followed by Dunn' multiple comparison test
502 correction (*p<0.05, **p<0.01, ****p<0.0001).
503
504 **Figure 5: CD37 N-terminus is involved in DuoHexaBody-CD37-mediated cytotoxic signaling**
505 (**A**) Histogram showing CD37 cell surface expression determined by flow cytometry analysis
506 of NALM6 cell lines expressing wild type CD37 (CD37-WT), or mutations of Tyr13 to
507 phenylalanine (CD37-Y13F), or deletion of Tyr13 (CD37-ΔY13) in the cytosolic regions of the
508 CD37 molecule. (**B**) p-AKT(S473) and (**C**) p-SHP1(Y564) on NALM6 cell lines transfected with
509 CD37-WT, CD37-Y13F or CD37-ΔY13 treated with DuoHexaBody-CD37 (DHB) and goat F(ab')2
510 anti-human IgG (a-Fc) or crosslinker alone (a-Fc). Dot plots depict p-AKT and p-SHP1 levels in
511 treated (DHB+a-Fc or a-Fc) vs untreated cells in CD37-GFP-positive (transfected) cells using
512 phosphoflow analysis, corrected for background signal from GFP-negative cells. Significance
513 was calculated using Student t-test (*p<0.05). Data shown from three independent
514 experiments.
515
516 **Figure 6: DuoHexaBody-CD37 treatment decreases cytokine-mediated pro-survival**
517 **signaling in DLBCL cell lines**
518 (**A**) Percentages of p-STAT6-positive cells (mean and SD) upon recombinant human IL-4 (rh-IL-
519 4) stimulation in DLBCL cells pre-treated with DuoHexaBody-CD37 in presence or absence of
520 goat F(ab')2 anti-human IgG (a-Fc). Data is shown from at least three independent
521 experiments. Percentages of p-STAT3-positive cells (mean +/- SD) upon (**B**) recombinant
522 human IL-6 (rh-IL-6) stimulation or (**C**) recombinant human IL-21 (rh-IL-21) stimulation in
523 DLBCL cells pre-treated with DuoHexaBody-CD37 in presence or absence of a-Fc. Data is
524 shown from at least three independent experiments. (**A-C**) Significance was calculated

525 compared to untreated control using Kruskal-Wallis test followed by Dunn' multiple
526 comparison test correction (**p<0.01).
527
528 **Supplementary Figure 1: Principal component analysis of (phospho)protein expression**
529 **profiles after DuoHexaBody-CD37 treatment**
530 Principal component analysis (PCA) of 484 proteins (102 phospho targets and 382 total
531 proteins) in primary B cells (CD19+ purified) and two DLBCL cell lines (Oci-Ly7 and U2932)
532 either untreated or treated with DuoHexaBody-CD37 in presence or absence of a-Fc using
533 reverse phase protein array (RPPA). The first two components of the cluster analysis are
534 shown.
535
536 **Supplementary Figure 2: DuoHexaBody-CD37 treatment results in differential activation of**
537 **BCR and RAS/MAPK downstream signaling proteins in B cells and DLBCL**
538 **(A-C)** Phosphoflow analysis of (A) p-SYK(Y348), p-SHP1(Y564), p-AKT(S473); **(B)** p-BTK(Y223),
539 p-PLCy2(Y759), p-PKCα/βII(T638/641) and **(C)** p38(T180/Y182), p-ERK-1/2(T202/Y204) on
540 primary B cells (*top row*) or DLBCL cells (*bottom row*) either anti-IgM treated or treated with
541 DuoHexaBody-CD37 and/or goat F(ab')2 anti-human IgG (a-Fc). Dot plots depict fold change
542 (mean +/- SD) of mean fluorescence intensity (MFI) of indicated treatment to untreated
543 cells. Each dot represents individual donor (B cells) or experimental replicate (DLBCL).
544 Significance of fold change to untreated control was calculated using Wilcoxon Signed Rank
545 test (*p<0.05, **p<0.01, ****p<0.0001).
546

547 **References**

548 1. Morin RD, Arthur SE, Hodson DJ. Molecular profiling in diffuse large B-cell lymphoma:
549 why so many types of subtypes? Br J Haematol. 2022;196(4):814–29.
550 2. Abou Dalle I, Dulery R, Moukalled N, Ricard L, Stocker N, El-Cheikh J, et al. Bi- and Tri-
551 specific antibodies in non-Hodgkin lymphoma: current data and perspectives. Blood
552 Cancer J. 2024;14(1).
553 3. Johnson NA, Boyle M, Bashashati A, Leach S, Brooks-Wilson A, Sehn LH, et al. Diffuse
554 large B-cell lymphoma: Reduced CD20 expression is associated with an inferior
555 survival. Blood. 2009;113(16):3773–80.
556 4. Xu-Monette ZY, Li L, Byrd JC, Jabbar KJ, Manyam GC, De Winde CM, et al. Assessment
557 of CD37 B-cell antigen and cell of origin significantly improves risk prediction in diffuse
558 large B-cell lymphoma. Blood. 2016;128(26):3083–100.
559 5. Guan XW, Wang HQ, Ban WW, Chang Z, Chen HZ, Jia L, et al. Novel HDAC inhibitor
560 Chidamide synergizes with Rituximab to inhibit diffuse large B-cell lymphoma tumour
561 growth by upregulating CD20. Cell Death Dis. 2020;11(1).
562 6. Roschewski M, Staudt LM, Wilson WH. Diffuse large B-cell lymphoma—treatment
563 approaches in the molecular era. Nat Rev Clin Oncol. 2013;11(1):12–23.
564 7. Varma G, Goldstein J, Advani RH. Novel agents in relapsed/refractory diffuse large B-
565 cell lymphoma. Hematol Oncol. 2023;41(S1):92–106.
566 8. Schwartz-Albiez R, Dörken B, Hofmann W, Moldenhauer G. The B cell-associated CD37
567 antigen (gp40-52). Structure and subcellular expression of an extensively glycosylated
568 glycoprotein. J Immunol 1988;140(3):905–14.
569 9. Van Spriel AB, De Keijzer S, Van Der Schaaf A, Gartlan KH, Sofi M, Light A, et al. The
570 tetraspanin CD37 orchestrates the α4β1 integrin-Akt signaling axis and supports long-

571 lived plasma cell survival. Sci Signal. 2012 ;5(250):ra82.

572 10. de Winde CM, Zuidscherwoude M, Vasaturo A, van der Schaaf A, Figdor CG, van Spriel
573 AB. Multispectral imaging reveals the tissue distribution of tetraspanins in human
574 lymphoid organs. Histochem Cell Biol. 2015; 144(2):133-46.

575 11. Berditchevski F, Rubinstein E. Tetraspanins. 2013. 1–418 p.
576 http://link.springer.com/10.1007/978-94-007-6070-7

577 12. Hemler ME. Targeting of tetraspanin proteins — potential benefits and strategies. Nat
578 Rev Drug Discov. 2008;7(9):747–58.

579 13. Querol Cano L, Dunlock VME, Schwerdtfeger F, van Spriel AB. Membrane organization
580 by tetraspanins and galectins shapes lymphocyte function. Nat Rev Immunol. 2024
581 ;24(3):193–212.

582 14. Barrena S, Almeida J, Yunta M, Lopez A, Fernandez-Mosteirin N, Giralt M, et al.
583 Aberrant expression of tetraspanin molecules in B-cell chronic lymphoproliferative
584 disorders and its correlation with normal B-cell maturation. Leukemia.
585 2005;19(8):1376–83.

586 15. Bobrowicz M, Kubacz M, Slusarczyk A, Winiarska M. Cd37 in b cell derived tumors—
587 more than just a docking point for monoclonal antibodies. Int J Mol Sci. 2020
588 ;21(24):1–16.

589 16. Beckwith KA, Byrd JC, Muthusamy N. Tetraspanins as therapeutic targets in
590 hematological malignancy: A concise review. Front Physiol. 2015 Mar 23;6.

591 17. De Winde CM, Veenbergen S, Young KH, Xu-Monette ZY, Wang XX, Xia Y, et al.
592 Tetraspanin CD37 protects against the development of B cell lymphoma. J Clin Invest.
593 2016;126(2):653–66.

594 18. Hashwah H, Bertram K, Stirm K, Stelling A, Wu C, Kasser S, et al. The IL-6 signaling

595 complex is a critical driver, negative prognostic factor, and therapeutic target in
596 diffuse large B-cell lymphoma . EMBO Mol Med. 2019;11(10).
597 19. Deckert J, Park PU, Chicklas S, Yi Y, Li M, Lai KC, et al. A novel anti-CD37 antibody-drug
598 conjugate with multiple anti-tumor mechanisms for the treatment of B-cell
599 malignancies. Blood. 2013;122(20):3500–10.
600 20. Beckwith KA, Frissora FW, Stefanovski MR, Towns WH, Cheney C, Mo X, et al. The
601 CD37-targeted antibody-drug conjugate IMGN529 is highly active against human CLL
602 and in a novel CD37 transgenic murine leukemia model. Leukemia. 2014; 144(2):133-
603 46.
604 21. Köksal H, Dillard P, Josefsson SE, Maggadottir SM, Pollmann S, Fane A, et al. Preclinical
605 development of CD37CAR T-cell therapy for treatment of B-cell lymphoma. Blood Adv.
606 2019;3(8):1230–43.
607 22. Imai K, Takeuchi Y, Terakura S, Okuno S, Adachi Y, Osaki M, et al. Dual CAR-T Cells
608 Targeting CD19 and CD37 Are Effective in Target Antigen Loss B-cell Tumor Models.
609 Mol Cancer Ther. 2024;23(3):381–93.
610 23. Caulier B, Joaquina S, Gelebart P, Dowling TH, Kaveh F, Thomas M, et al. CD37 is a safe
611 chimeric antigen receptor target to treat acute myeloid leukemia. Cell Reports Med.
612 2024;5(6).
613 24. Witkowska M, Smolewski P, Robak T. Investigational therapies targeting CD37 for the
614 treatment of B-cell lymphoid malignancies. Expert Opin Investig Drugs.
615 2018;27(2):171–7.
616 25. Oostindie SC, Van Der Horst HJ, Kil LP, Strumane K, Overdijk MB, Van Den Brink EN, et
617 al. DuoHexaBody-CD37 ® , a novel biparatopic CD37 antibody with enhanced Fc-
618 mediated hexamerization as a potential therapy for B-cell malignancies. Blood Cancer

619 J. 2020;10:30.
620 26. van der Horst HJ, Oostindie SC, Cillessen SAGM, Gelderloos AT, Overdijk MB, Nijhof IS,
621 et al. Potent Preclinical Efficacy of DuoHexaBody-CD37 in B-Cell Malignancies.
622 HemaSphere. 2021;5(1):e504.
623 27. Lapalombella R, Yeh YY, Wang L, Ramanunni A, Rafiq S, Jha S, et al. Tetraspanin CD37
624 directly mediates transduction of survival and apoptotic signals. Cancer Cell.
625 2012;21(5):694–708.
626 28. Fujimura T, Yamashita-Kashima Y, Kawasaki N, Yoshiura S, Harada N, Yoshimura Y.
627 Obinutuzumab in combination with chemotherapy enhances direct cell death in cd20-
628 positive obinutuzumab-resistant non-hodgkin lymphoma cells. Mol Cancer Ther. 2021
629 ;20(6):1133–41.
630 29. Mone AP, Cheney C, Banks AL, Tridandapani S, Mehter N, Guster S, et al.
631 Alemtuzumab induces caspase-independent cell death in human chronic lymphocytic
632 leukemia cells through a lipid raft-dependent mechanism. Leukemia. 2006;20:272–9.
633 30. Zhao X, Lapalombella R, Joshi T, Cheney C, Gowda A, Hayden-Ledbetter MS, et al.
634 Targeting CD37-positive lymphoid malignancies with a novel engineered small
635 modular immunopharmaceutical. Blood 2007;110(7):2569–77.
636 31. Beers SA, French RR, Chan HTC, Lim SH, Jarrett TC, Vidal RM, et al. Antigenic
637 modulation limits the efficacy of anti-CD20 antibodies: Implications for antibody
638 selection. Blood. 2010;115(25):5191–201.
639 32. Lim SH, Vaughan AT, Ashton-Key M, Williams EL, Dixon S V., Chan HTC, et al. Fc
640 gamma receptor IIb on target B cells promotes rituximab internalization and reduces
641 clinical efficacy. Blood. 2011;118(9):2530–40.
642 33. Whittaker KC, Huang RP. Antibody Arrays Methods and Protocols. 2021. 45–54 p.

643 Available from: http://www.springer.com/series/7651

644 34. Pal Singh S, Dammeijer F, Hendriks RW. Role of Bruton's tyrosine kinase in B cells and
645 malignancies. Mol Cancer. 2018;17(1):1–23.

646 35. Benoit A, Bou-Petit E, Chou H, Lu M, Guilbert C, Luo VM, et al. Mutated RAS-
647 associating proteins and ERK activation in relapse/refractory diffuse large B cell
648 lymphoma. Sci Rep. 2022;12(1).

649 36. Uddin S, Hussain AR, Siraj AK, Manogaran PS, Al-Jomah NA, Moorji A, et al. Role of
650 phosphatidylinositol 3'-kinase/AKT pathway in diffuse large B-cell lymphoma survival.
651 Blood. 2006;108(13):4178–86.

652 37. Höpken UE, Rehm A. Targeting the Tumor Microenvironment of Leukemia and
653 Lymphoma. Trends in Cancer. 2019;5(6):351–64.

654 38. Wang Y, Wang C, Cai X, Mou C, Cui X, Zhang Y, et al. IL-21 Stimulates the expression
655 and activation of cell cycle regulators and promotes cell proliferation in EBV-positive
656 diffuse large B cell lymphoma. Sci Rep. 2020;10(1):1–13.

657 39. Jones ELL, Demaria MCC, Wright MDD. Tetraspanins in cellular immunity. Biochem Soc
658 Trans. 2011;39(2):506–11.

659 40. Wood B, Sikdar S, Choi SJ, Virk S, Alhejaily A, Baetz T, et al. Leukemia & Lymphoma
660 Abundant expression of interleukin-21 receptor in follicular lymphoma cells is
661 associated with more aggressive disease Abundant expression of interleukin-21
662 receptor in follicular lymphoma cells is associated with more aggressive disease. Leuk
663 Lymphoma. 2013;54(6):1212–20.

664 41. Zöller M. Tetraspanins: Push and pull in suppressing and promoting metastasis. Nat
665 Rev Cancer. 2009;9(1):40–55.

666 42. Kumari S, Devi G V, Badana anil, ramesh Dasari V, rao malla rama. CD151-A Striking

667 Marker for Cancer Therapy. Biomark Cancer. 2015;(7):7–7.
668 43. Vences-Catalán F, Kuo CC, Rajapaksa R, Duault C, Andor N, Czerwinski DK, et al. CD81
669 is a novel immunotherapeutic target for B cell lymphoma. J Exp Med. 2019
670 ;jem.20190186.
671 44. Yoshimura T, Miyoshi H, Shimono J, Nakashima K, Takeuchi M, Yanagida E, et al. CD37
672 expression in follicular lymphoma. Ann Hematol. 2022;101(5):1067–75.
673 45. Roumenina LT, Daugan M V., Noe R, Petitprez F, Vano YA, Sanchez-Salas R, et al.
674 Tumor cells hijack macrophage-produced complement C1q to promote tumor growth.
675 Cancer Immunol Res. 2019;7(7):1091–105.
676 46. Nemenoff RA, Markiewski MM. The role of complement in the tumor
677 microenvironment Fac Rev. 2021;10(80).
678 47. Luo S, Wang M, Wang H, Hu D, Zipfel PF, Hu Y. How Does Complement Affect
679 Hematological Malignancies: From Basic Mechanisms to Clinical Application. Front
680 Immunol. 2020;11.
681 48. Song G, Cho WC, Gu L, He B, Pan Y, Wang S. Increased CD59 protein expression is
682 associated with the outcome of patients with diffuse large B-cell lymphoma treated
683 with R-CHOP. Med Oncol. 2014;31(7).
684 49. Fowler NH, Cheah CY, Gascoyne RD, Gribben J, Neelapu SS, Ghia P, et al. Role of the
685 tumor microenvironment in mature B-cell lymphoid malignancies. Haematologica.
686 2016;101(5):531–40.
687 50. Singhal S, Rao AS, Stadanlick J, Bruns K, Sullivan NT, Bermudez A, et al. Human Tumor–
688 Associated Macrophages and Neutrophils Regulate Antitumor Antibody Efficacy
689 through Lethal and Sublethal Trogocytosis. Cancer Res. 2024 ;84(7):1029–47.
690 51. Bouwstra R, He Y, De Boer J, Kooistra H, Cendrowicz E, Fehrmann RSN, et al. CD47

691 expression defines efficacy of rituximab with CHOP in non–germinal center B-cell
692 (Non-GCB) diffuse large B-cell lymphoma patients (DLBCL), but not in GCB DLBCL.
693 Cancer Immunol Res. 2019 ;7(10):1663–71.
694 52. Zhao X, Lapalombella R, Joshi T, Cheney C, Gowda A, Hayden-Ledbetter MS, et al.
695 Targeting CD37-positive lymphoid malignancies with a novel engineered small
696 modular immunopharmaceutical. Blood. 2007;110(7):2569–77.
697 53. Rafiq S, Siadak A, Butchar JP, Cheney C, Lozanski G, Jacob NK, et al. Glycovariant anti-
698 CD37 monospecific protein therapeutic exhibits enhanced effector cell-mediated
699 cytotoxicity against chronic and acute B cell malignancies. MAbs. 2013;5(5):723–35.
700 54. Wang J, Xu-Monette ZY, Jabbar KJ, Shen Q, Manyam GC, Tzankov A, et al. AKT
701 Hyperactivation and the Potential of AKT-Targeted Therapy in Diffuse Large B-Cell
702 Lymphoma. Am J Pathol 2017;187:1700–16.
703 55. Arribas A, Napoli S, Munz N, Stussi G, Bertoni F. PI3Kδ activation, IL6 over-expression,
704 and CD37 loss cause resistance to naratuximab emtansine in lymphomas. Blood Adv.
705 2024; bloodadvances.2023012291
706 56. Krause G, Baki I, Kerwien S, Knödgen E, Neumann L, Göckeritz E, et al. Cytotoxicity of
707 the CD37 antibody BI 836826 against chronic lymphocytic leukaemia cells in
708 combination with chemotherapeutic agents or PI3K inhibitors. Br J Haematol.
709 2016;173(5):791–4.
710 57. Rødland GE, Melhus K, Generalov R, Gilani S, Bertoni F, Dahle J, et al. The Dual Cell
711 Cycle Kinase Inhibitor JNJ-7706621 Reverses Resistance to CD37-Targeted
712 Radioimmunotherapy in Activated B Cell Like Diffuse Large B Cell Lymphoma Cell
713 Lines. Front Oncol. 2019;9:1301.
714 58. Wilson WH, Young RM, Schmitz R, Yang Y, Pittaluga S, Wright G, et al. Targeting B cell

715 receptor signaling with ibrutinib in diffuse large B cell lymphoma. Nat Med.
716 2015;21(8).
717 59. Wilson WH, Wright GW, Huang DW, Hodkinson B, Balasubramanian S, Fan Y, et al.
718 Effect of ibrutinib with R-CHOP chemotherapy in genetic subtypes of DLBCL. Cancer
719 Cell. 2021;39(12):1643-1653.e3.
720 60. Oostindie SC, Taylor RP, Van Der Horst HJ, Lindorfer MA, Cook EM, Tupitza JC, et al.
721 CD20 and CD37 antibodies synergize to activate complement by Fc-mediated
722 clustering. Haematologica. 2019 ;104(9):1841.
723

Figure 1

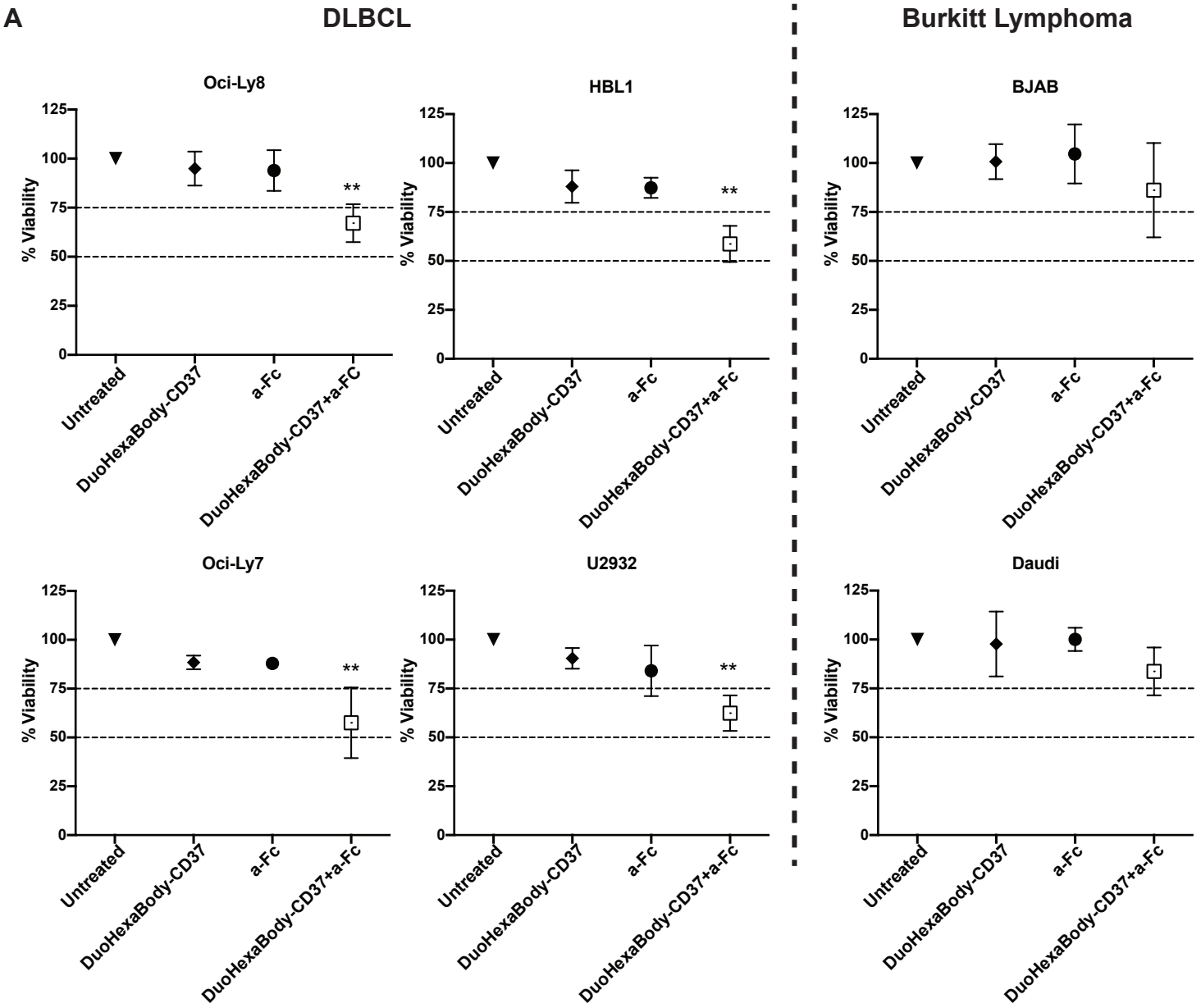
A
DLBCL
Burkitt Lymphoma
Oci-Ly8
HBL1
BJAB
Oci-Ly7
U2932
Daudi
% Viability
125
100
75
50
25
0
**
Untreated
DuoHexaBody-CD37
a-Fc
DuoHexaBody-CD37+a-Fc

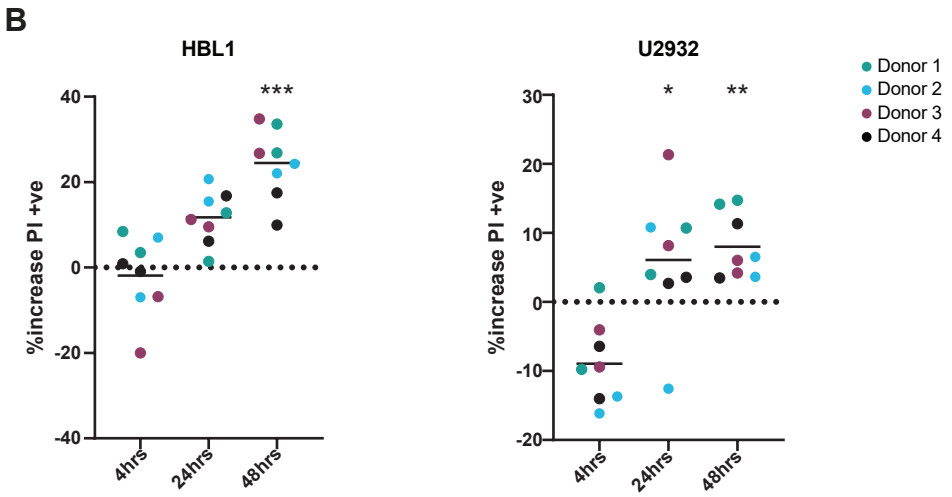
B
HBL1
U2932
%increase PI +ve
40
20
0
-20
-40
30
10
-10
***
*
**
4hrs
24hrs
48hrs
Donor 1
Donor 2
Donor 3
Donor 4

Figure 2

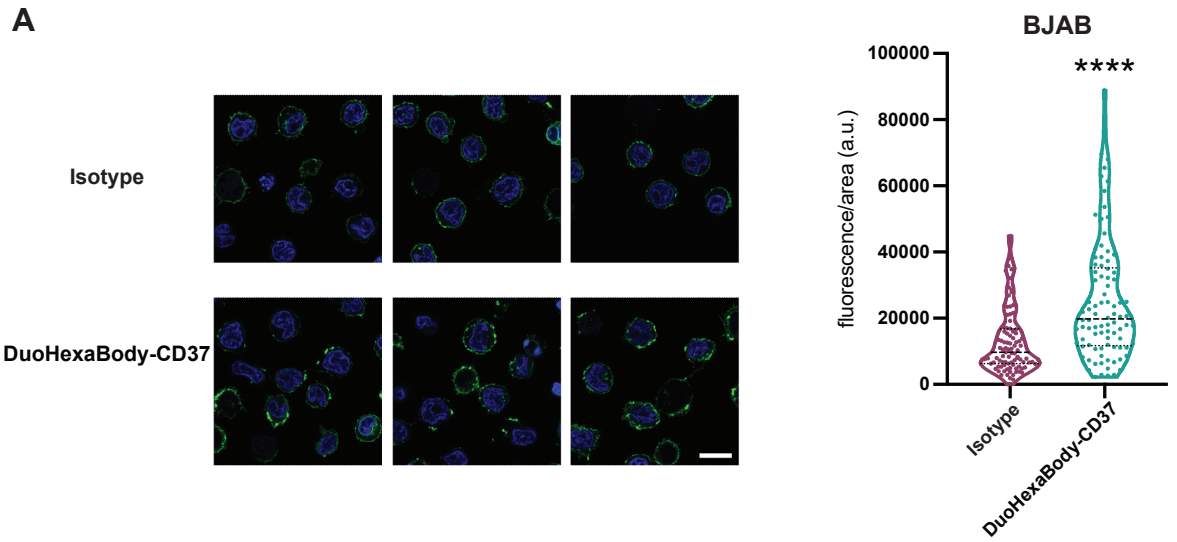
A
Isotype
DuoHexaBody-CD37
BJAB
****
fluorescence/area (a.u.)
100000
80000
60000
40000
20000
0
Isotype
DuoHexaBody-CD37

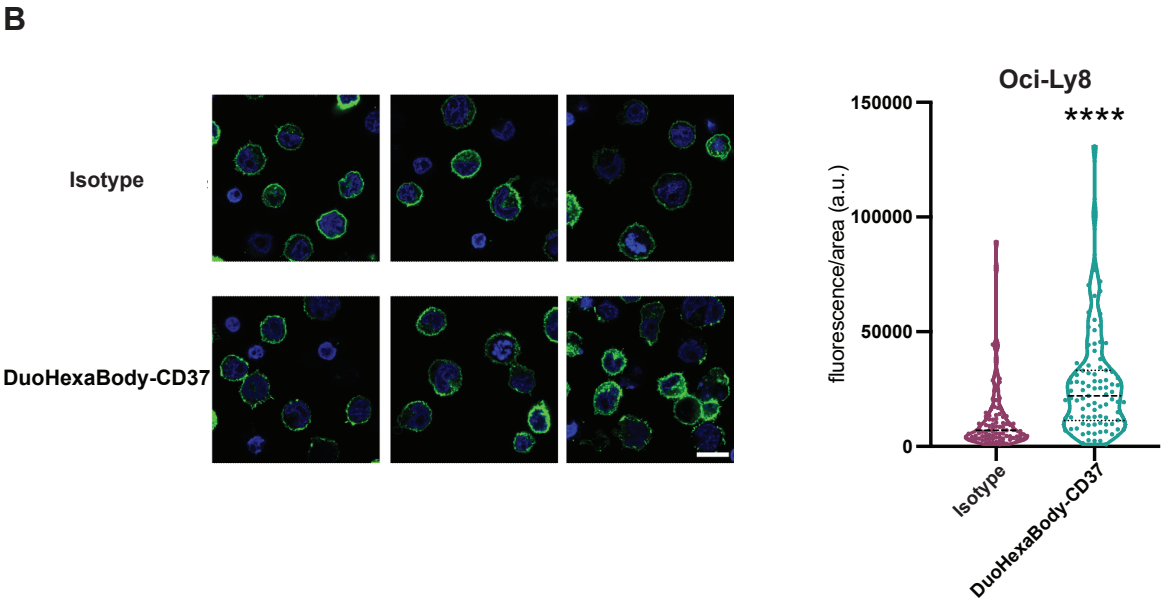
B
Isotype
DuoHexaBody-CD37
Oci-Ly8
****
fluorescence/area (a.u.)
150000
100000
50000
0
Isotype
DuoHexaBody-CD37

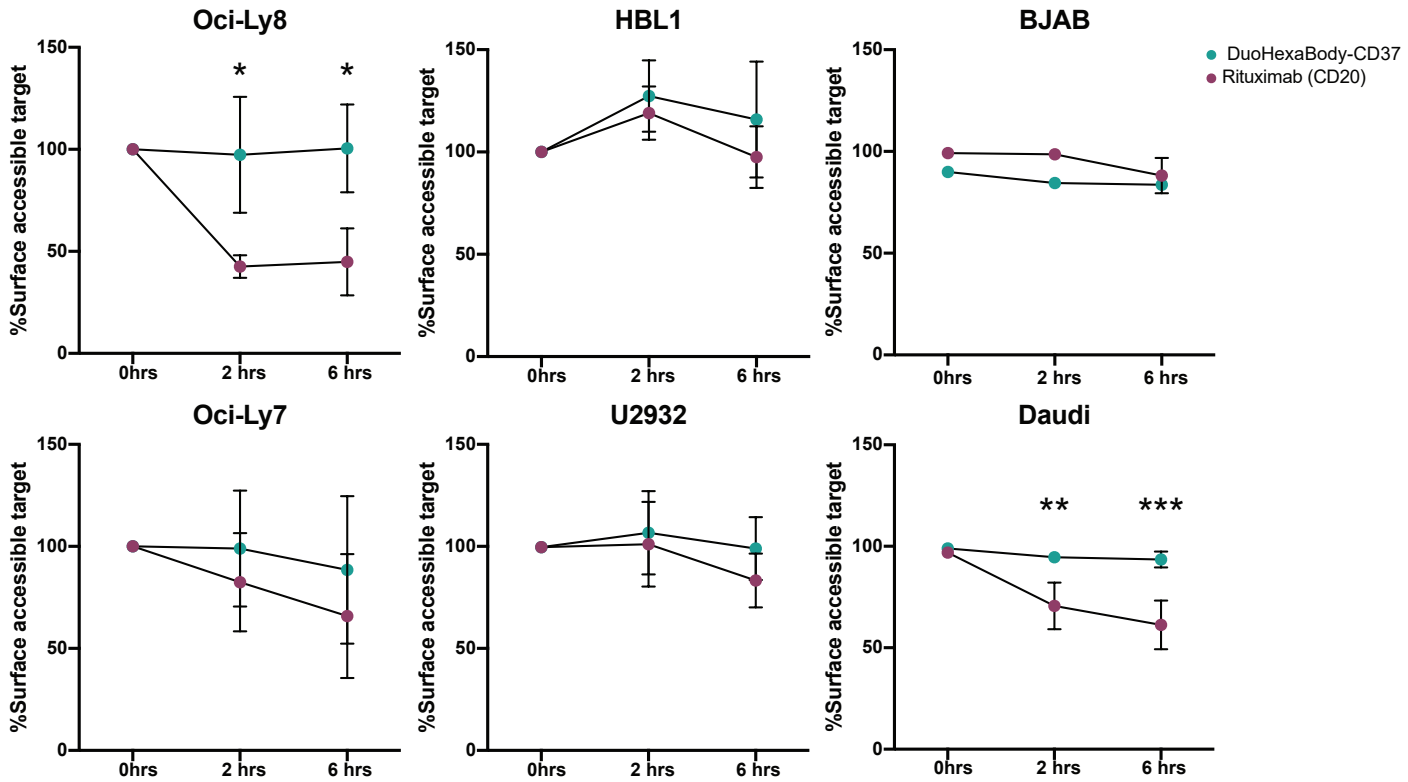
C
Oci-Ly8
HBL1
BJAB
Oci-Ly7
U2932
Daudi
DuoHexaBody-CD37
Rituximab (CD20)
%Surface accessible target
150
100
50
0
0hrs
2 hrs
6 hrs
*
*
**
***

Figure 3

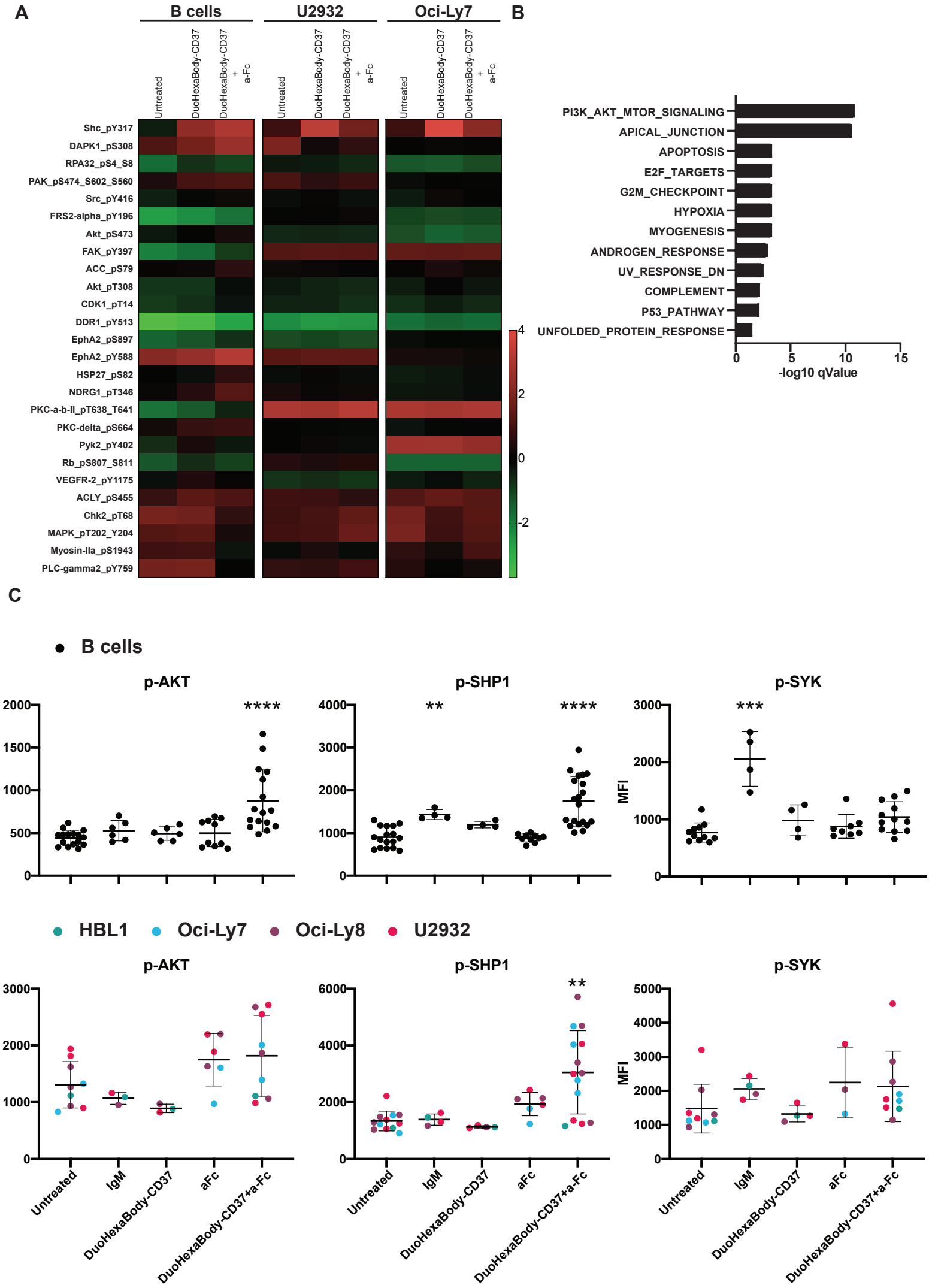
A
B cells
U2932
Oci-Ly7
Untreated
DuoHexaBody-CD37
DuoHexaBody-CD37 + a-Fc
Shc_pY317
DAPK1_pS308
RPA32_pS4_S8
PAK_pS474_S602_S560
Src_pY416
FRS2-alpha_pY196
Akt_pS473
FAK_pY397
ACC_pS79
Akt_pT308
CDK1_pT14
DDR1_pY513
EphA2_pS897
EphA2_pY588
HSP27_pS82
NDRG1_pT346
PKC-a-b-II_pT638_T641
PKC-delta_pS664
Pyk2_pY402
Rb_pS807_S811
VEGFR-2_pY1175
ACLY_pS455
Chk2_pT68
MAPK_pT202_Y204
Myosin-IIa_pS1943
PLC-gamma2_pY759
4
2
0
-2
B
PI3K_AKT_MTOR_SIGNALING
APICAL_JUNCTION
APOPTOSIS
E2F_TARGETS
G2M_CHECKPOINT
HYPOXIA
MYOGENESIS
ANDROGEN_RESPONSE
UV_RESPONSE_DN
COMPLEMENT
P53_PATHWAY
UNFOLDED_PROTEIN_RESPONSE
0
5
10
15
-log10 qValue
C
B cells
p-AKT
p-SHP1
p-SYK
MFI
****
**
****
***
HBL1
Oci-Ly7
Oci-Ly8
U2932
p-AKT
p-SHP1
p-SYK
**
Untreated
IgM
DuoHexaBody-CD37
aFc
DuoHexaBody-CD37+a-Fc

Figure 4

A

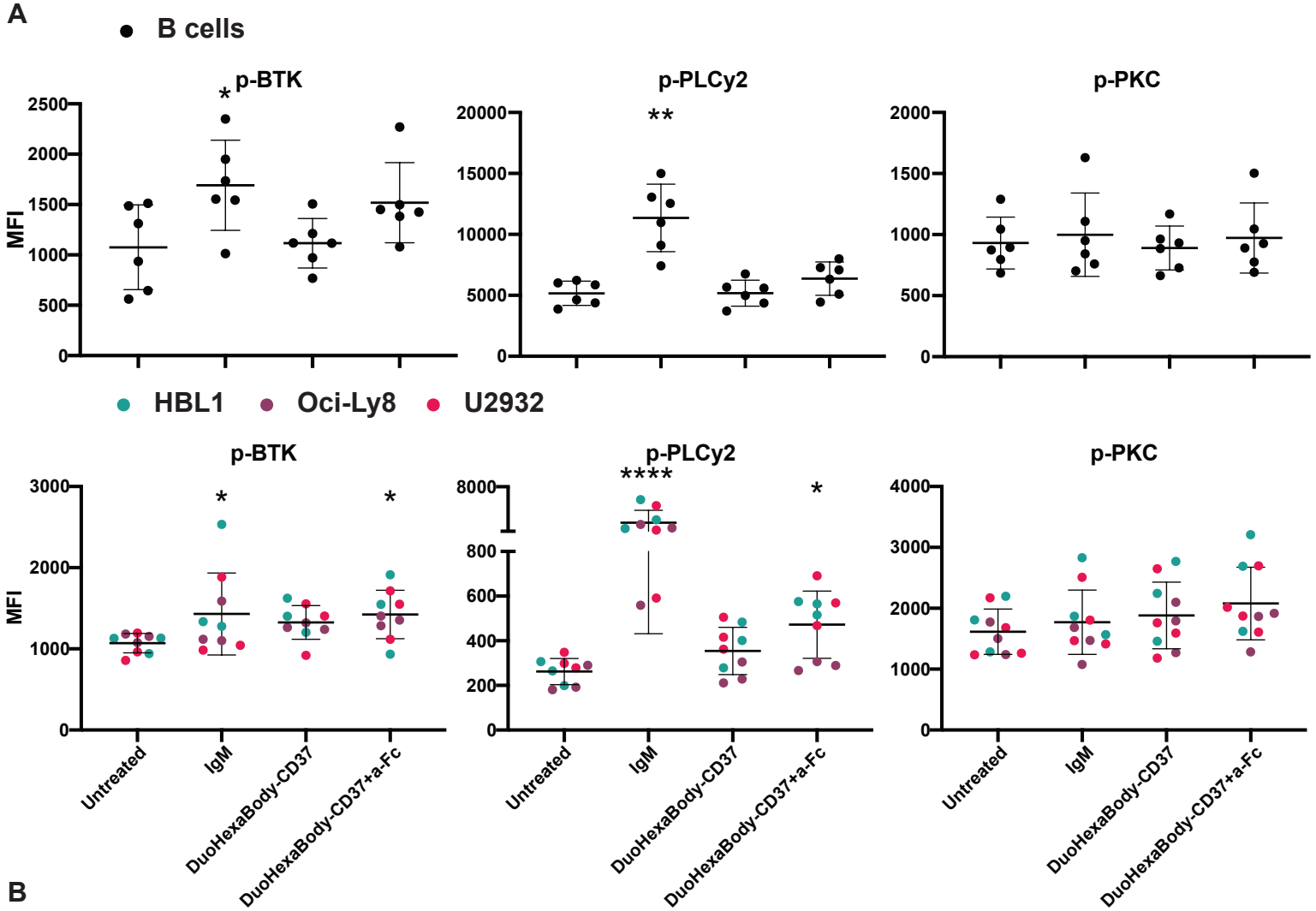
B cells
p-BTK
p-PLCy2
p-PKC
MFI
HBL1
Oci-Ly8
U2932
Untreated
IgM
DuoHexaBody-CD37
DuoHexaBody-CD37+a-Fc

B

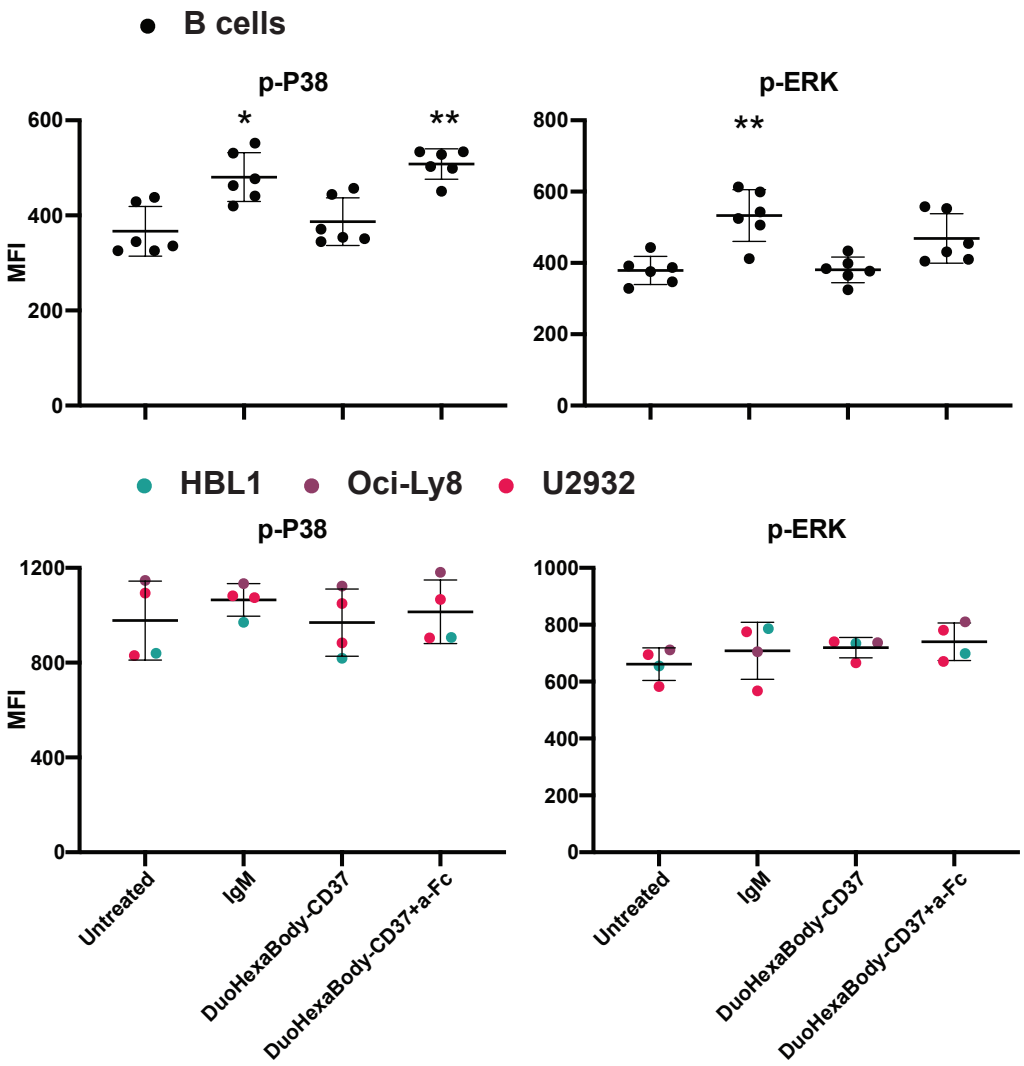
B cells
p-P38
p-ERK
MFI
HBL1
Oci-Ly8
U2932
Untreated
IgM
DuoHexaBody-CD37
DuoHexaBody-CD37+a-Fc

Figure 5

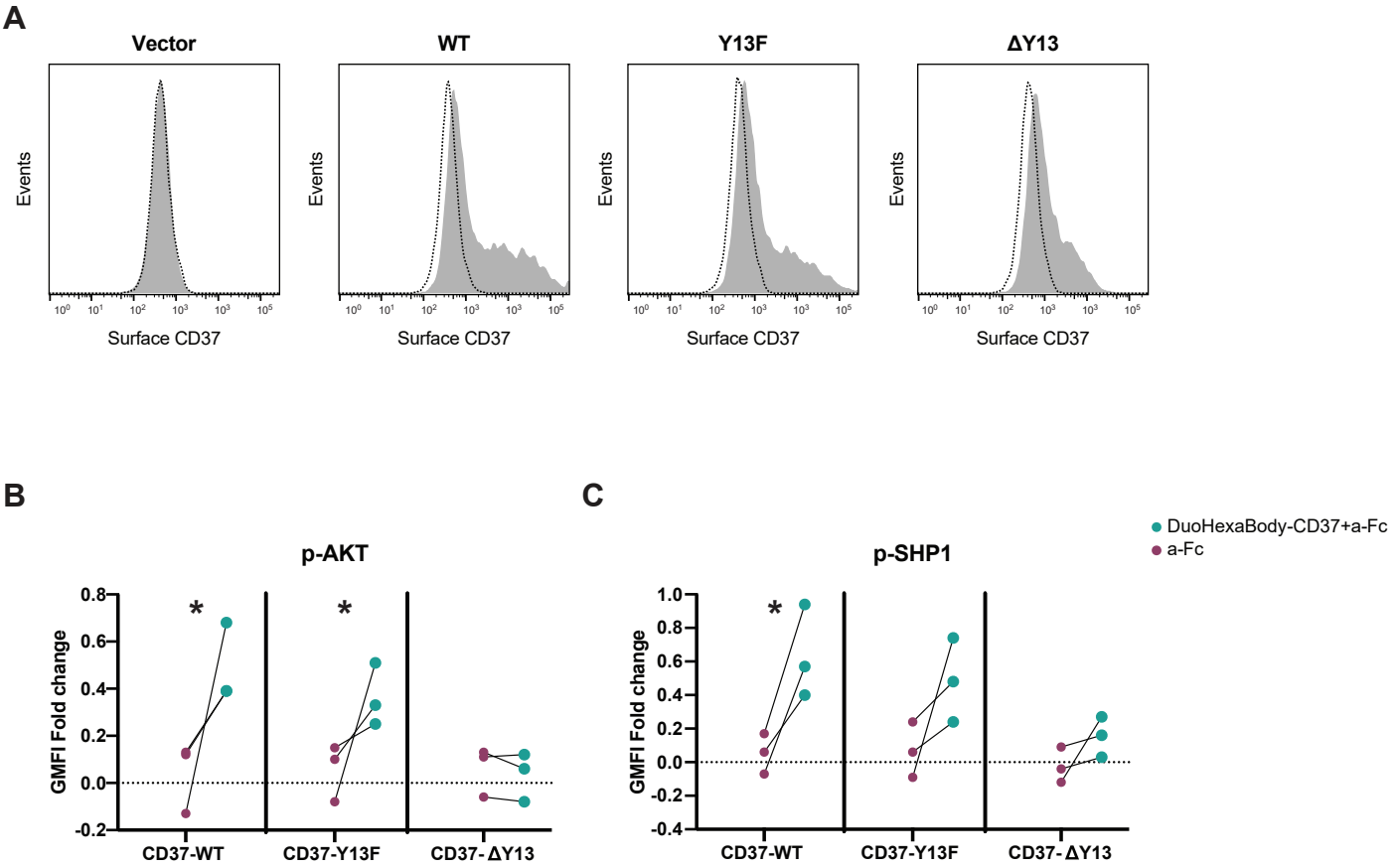
A
Vector
WT
Y13F
ΔY13
Events
Surface CD37
B
p-AKT
GMFI Fold change
0.8
0.6
0.4
0.2
0.0
-0.2
*
*
CD37-WT
CD37-Y13F
CD37-ΔY13
C
p-SHP1
GMFI Fold change
1.0
0.8
0.6
0.4
0.2
0.0
-0.2
-0.4
*
CD37-WT
CD37-Y13F
CD37-ΔY13
DuoHexaBody-CD37+a-Fc
a-Fc

Figure 6

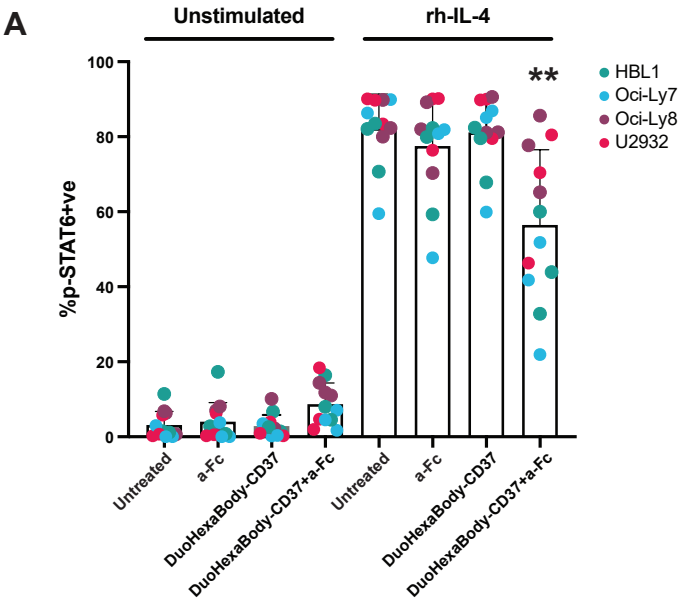
A
Unstimulated
rh-IL-4
%p-STAT6+ve
100
80
60
40
20
0
**
HBL1
Oci-Ly7
Oci-Ly8
U2932
Untreated
a-Fc
DuoHexaBody-CD37
DuoHexaBody-CD37+a-Fc
Untreated
a-Fc
DuoHexaBody-CD37
DuoHexaBody-CD37+a-Fc

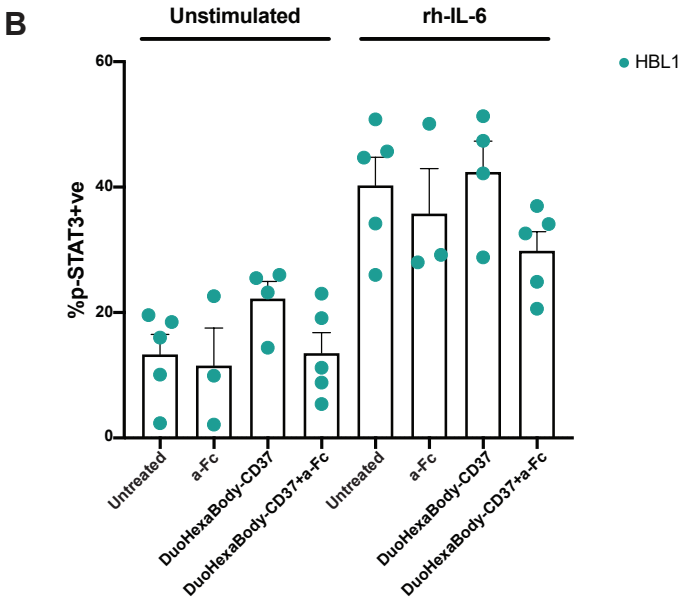
B
Unstimulated
rh-IL-6
%p-STAT3+ve
60
40
20
0
HBL1
Untreated
a-Fc
DuoHexaBody-CD37
DuoHexaBody-CD37+a-Fc
Untreated
a-Fc
DuoHexaBody-CD37
DuoHexaBody-CD37+a-Fc

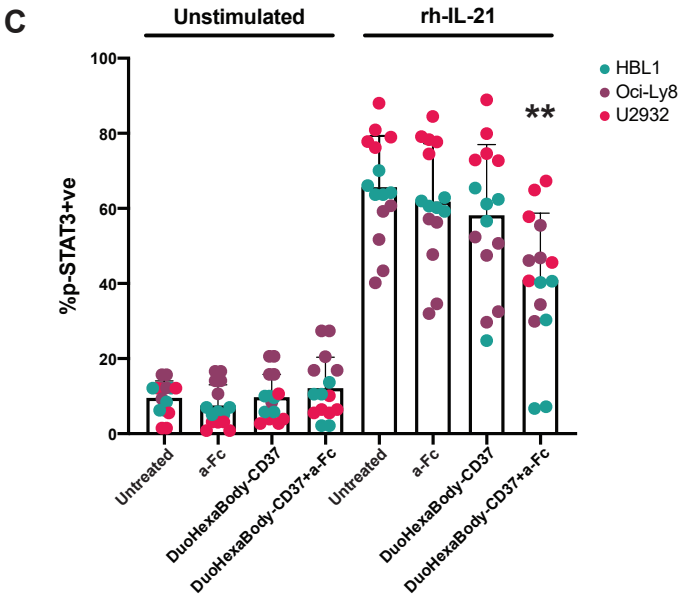
C
Unstimulated
rh-IL-21
%p-STAT3+ve
100
80
60
40
20
0
**
HBL1
Oci-Ly8
U2932
Untreated
a-Fc
DuoHexaBody-CD37
DuoHexaBody-CD37+a-Fc
Untreated
a-Fc
DuoHexaBody-CD37
DuoHexaBody-CD37+a-Fc